Z. Physik B – Condensed Matter 39, 299–304 (1980)

Condensed Matter
Zeitschrift für Physik B

The Elastic Behaviour of Ferroelastic Sb_5O_7I Polytype 2MC Studied by Ultrasonic Experiments* and Brillouin Scattering**

W. Rehwald and A. Vonlanthen
Laboratories RCA Ltd, Zürich, Switzerland

E. Rehaber and W. Prettl
Fakultät für Physik der Universität, Regensburg, Federal Republic of Germany

Received May 12, 1980

The temperature dependence of the elastic functions of the improper ferroelastic polytype 2MC – Sb_5O_7I has been investigated in the temperature range from room temperature to well above the structural phase transition at $T_c = 481$ K. The stiffnesses $c(c^*c^*)$, $c(a,a)$, c_{22} and $c(c^*a)$ show a considerable softening up to 20% around T_c whereas c_{44} remains unaffected by the phase transition. The experimental results are discussed considering cubic and quartic anharmonic coupling between two components of the zone boundary order parameter and elastic waves.

1. Introduction

At room temperature pentaantimony heptaoxide-iodide, Sb_5O_7I, shows the properties of a ferroelastic material: By applying uniaxial compression the crystal can be switched into one of the three possible domains or orientational states [1]. By this procedure we also can obtain monodomain samples and eliminate all the difficulties arising from domains, which hamper many physical investigations around phase transition points. Ultrasonic measurements usually probe a sizeable volume and are especially plagued by domain effects. Therefore Sb_5O_7I seems to be a favourable candidate for studying the elastic behaviour in the ordered phase by ultrasonic techniques as well as by Brillouin scattering.

Crystals of Sb_5O_7I exhibit polytypism [2]. Here we consider only the α- or 2MC-polytype. It transforms at $T_c = 481$ K from a hexagonal high temperature phase C_{6h}^2 (= P 6_3/m) into a ferroelastic, non-ferroelectric monoclinic phase of space group C_{2h}^5 (= P 2_1/c). By x-ray diffraction it has been demonstrated that in the transition to monoclinic symmetry not only the 120° angle between two axes changes, but also the unit cell doubles in one direction (monoclinic c-direction) [3]. This means that the order parameter has a wavevector

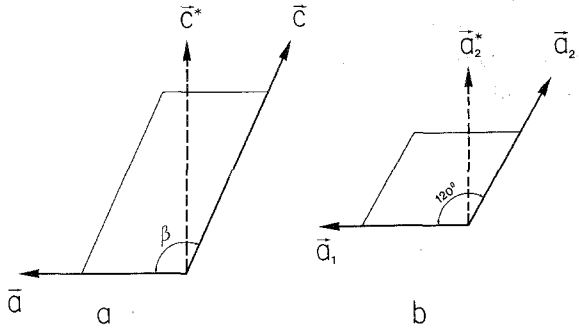

Fig. 1. Unit cell and basis vectors for the direct and reciprocal lattice in the monoclinic *a* and hexagonal *b* phase

$\mathbf{q_M} = \mathbf{a}_2^*/2$ in hexagonal notation*, or its equivalent for the other two domain orientations [5]. Consequently the spontaneous strain is proportional to the square of the order parameter, rendering this material an improper ferroelastic.

In addition 2MC – Sb_5O_7I was studied intensively by Raman scattering [4, 5]. Special attention has been paid to the intensity of phonon modes forbidden in the hexagonal phase. From this and also from the observation of transition-induced optical birefringence [6] it has been concluded that the phase transition is weakly discontinuous (first order), but with a narrow

* Carried out in Laboratories RCA Ltd, Zürich, Switzerland
** Carried out in Fakultät für Physik der Universität, Regensburg, Federal Republic of Germany

* The basis vectors of the reciprocal lattice are denoted by a star. See Fig. 1

0340-224X/80/0039/0299/$01.20

Table 1. Sound wave stiffnesses $\rho v_s^2(\mathbf{n},\mathbf{e})$ in the hexagonal and monoclinic phases, following the choise of axes x‖a_1 or a; y‖a_2^* or b; z‖c or c*

Hexagonal (n,e)	ρv_s^2	Monoclinic (n,e)	ρv_s^2
(a_1,a_1)	c_{11}	$(a,a)_Q$	$\frac{c_{11}+c_{55}}{2}+\sqrt{\left(\frac{c_{11}-c_{55}}{2}\right)^2+c_{15}^2}$
(a_1,a_2^*)	$c_{66}=\frac{c_{11}-c_{12}}{2}$	$(a,c^*)_Q$	$\frac{c_{11}+c_{55}}{2}-\sqrt{\left(\frac{c_{11}-c_{55}}{2}\right)^2+c_{15}^2}$
(a_1,c)	c_{44}	(a,b)	c_{66}
(a_2^*,a_2^*)	c_{11}	$(c^*,c^*)_Q$	$\frac{c_{33}+c_{55}}{2}+\sqrt{\left(\frac{c_{33}-c_{55}}{2}\right)^2+c_{35}^2}$
(a_2^*,c)	c_{44}	(c^*,b)	c_{44}
(a_2^*,a_1)	$c_{66}=\frac{c_{11}-c_{12}}{2}$	$(c^*,a)_Q$	$\frac{c_{33}+c_{55}}{2}-\sqrt{\left(\frac{c_{33}-c_{55}}{2}\right)^2+c_{35}^2}$
(c,c)	c_{33}	(b,b)	c_{22}
(c,a_1)	c_{44}	$(b,a)_Q$	$\frac{c_{66}+c_{44}}{2}+\sqrt{\left(\frac{c_{66}-c_{44}}{2}\right)^2+c_{46}^2}$
(c,a_2^*)	c_{44}	$(b,c^*)_Q$	$\frac{c_{66}+c_{44}}{2}-\sqrt{\left(\frac{c_{66}-c_{44}}{2}\right)^2+c_{46}^2}$

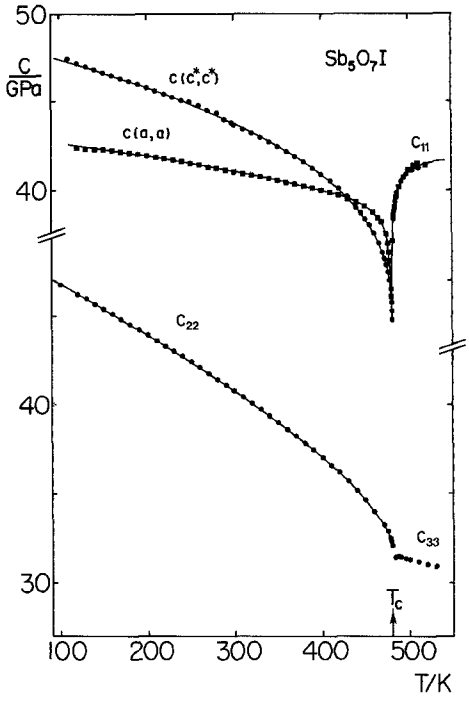

Fig. 2. Temperature variation of the stiffnesses belonging to longitudinal and quasi-longitudinal waves, measured by ultrasonic techniques. Full lines represent a computer fit to (3) for c_{11}, to (4) for c_{22}, to (5) for c(a,a) and a superposition of (4) and (5) for c(c*,c*). The nomenclature is according to Table 1

metastability region of $T_1 - T_0 \simeq 1$ K. The temperature dependence of the order parameter – a phonon coordinate involving predominantly the displacement of iodine atoms parallel to the c-plane – is well described by the Landau theory.

2. Experimental

2.1. Ultrasonic Measurements

The crystals used in all our investigations were grown by sublimation in a vertical temperature gradient in the Cristallographic Institute of the University of Freiburg [1]. For ultrasonic measurements the crystals were made monodomain by compressing them along the monoclinic c*-direction, and oriented either optically under a polarizing microscope or by x-rays on a Bragg goniometer. A pair of parallel faces were cut and polished to optical precision. One face was metallized with evaporated aluminium and an x- or y-cut quartz transducer having 15 or 30 MHz fundamental resonance frequency was bonded to it by epoxy resin.

By the puls-echo overlap method we tried to measure all the possible longitudinal, transverse, quasi-longitudinal, and quasi-transverse waves along the main axes a, b, and c* as a function of temperature in the range 100 K to 520 K. Using a constant mass density $\rho = 5550$ kg/m^3 [3] we converted the measured velocities into the corresponding elastic stiffnesses. The connection with the components c_{ij} of the stiffness tensor is given in Table 1 for the monoclinic and hexagonal phase. The choice of axes (a, b, c*) in the monoclinic phase does not obey the "IRE Standard on Piezoelectric Crystals" [7], but is more advantageous in this case.

Measuring the longitudinal or quasi-longitudinal wave did not pose any severe problems. The results are plotted in Fig. 2. However, we did not succed to determine the shearwave velocities over the whole temperature range. Invariably the signal amplitude decreased upon heating and diminished in most cases to unmeasurably small values around 400 K. Carrying the sample through the phase transition at 481 K did not restore the signal. In a few cases it was possible to measure up to 500 K, but the data obtained showed relatively strong variations around 400 K and were not reproducible. Our suspicion is that domains form in this temperature range, although the crystal has been made monodomain before the experiment. We tried to perform the measurement under more or less constant compression in a specially designed sample holder. By this we could extend the measurable temperature range by some 10 to 20 degrees, but were not able to reach T_c. The fact that above T_c no shear-wave

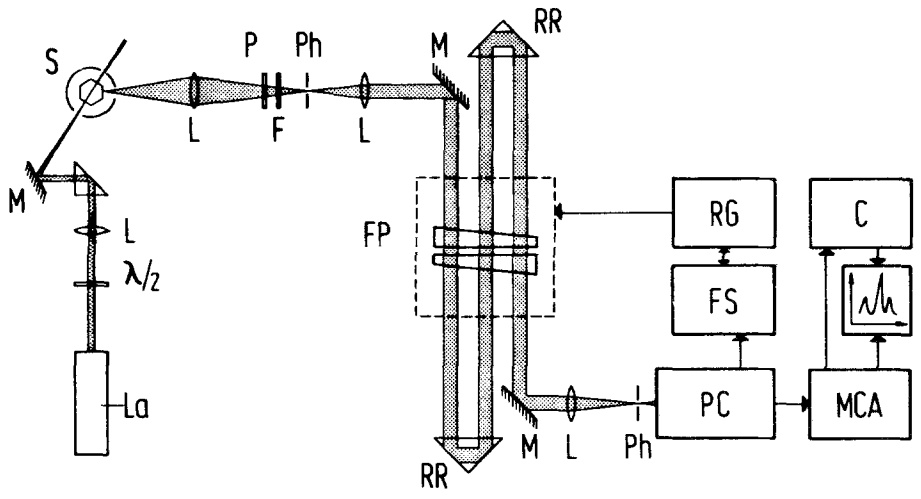

Fig. 3. General set up of the Brillouin scattering experiment; FP: Plane Fabry-Perot-Interferometer; RR: Retroreflector; S: Sample in a little copper oven; $\lambda/2$: Half wave plate; F: Interference filter; PC: Photon-counting equipment; MCA: Signal averager; FS: Finesse stabilizer; La: Laser; M: Mirror; L: Lens; P: Polarizer; Ph: Pinhole; RG: Ramp Generator; C: Computer

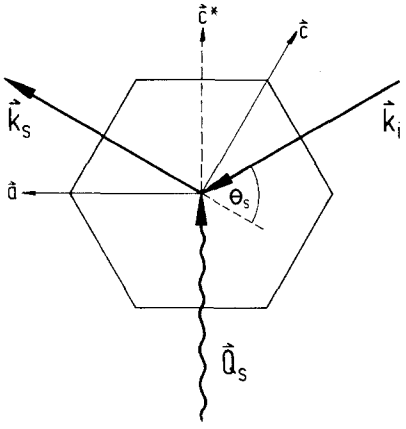

Fig. 4. Scattering geometry: $\mathbf{k}_i$, $\mathbf{k}_s$ and $\mathbf{Q}_s$ are the wavevectors of incident light, scattered light and the acoustic phonons, respectively, in the monoclinic (ac)-plane. $\theta_s = 60°$ is the scattering angle. Monoclinic crystallographic axes are shown relative to the hexagonal shape of as-grown crystals

measurements were possible is probably due to a partial bond breaking. Because of these difficulties we started to look at the transverse and quasi-transverse waves by Brillouin scattering.

The sample and its copper sample holder were placed inside an electric furnace. Two attached copper-constantan thermocouples served to measure the temperature and to operate an Eurotherm temperature controller. The sound velocities measured by the pulse-overlap technique also helped to determine the point where temperature stability had been reached. The accuracy of the temperature measurement is ± 0.5 K.

Pulse-overlap measurements have a high relative accuracy (better than $1:10^4$) but suffer in their absolute accuracy from an uncertainty to obtain the proper rf phase. Although there exist test procedures on the correct phase overlap [8], they do not work unless crystal and bond are sufficiently perfect. The error in the absolute value of the c_{ij} is consequently estimated ± 7 to 8%.

2.2. Brillouin Scattering

The experimental setup is displayed in Fig. 3. The excitation of the Brillouin spectra was provided by a 4 W single mode Argon laser. The laser beam was focused perpendicularly on a natural plane of prism shaped as-grown crystals of hexagonal cross section. The scattering geometry with respect to the orientation of the single domain crystal is shown in Fig. 4 in a projection on the scattering plane containing the a and c crystallographic axes of the monoclinic structure. The scattered light was analysed at a scattering angle of $\theta_s = 60°$ utilizing a piezo-scanned plane Fabry Perot interferometer. The device was used in a three-pass configuration. The finesse of the interferometer was stabilized by an electronic controller built by J. R. Sandercock [9]. The crystal was heated from room temperature up to 530 K in a little copper oven. The spectra were recorded with standard photon counting techniques and a signal averaging system.

A typical scattering spectrum is shown in Fig. 5. All three acoustic modes could be observed for the whole temperature range (300–530 K). We calculated the stiffnesses from the measured frequency shifts using the mass density given above and $n = 2.3$ for the refractive index [2]. The resulting temperature dependence of the elastic constants is plotted in Fig. 6. The scattering configuration used here yielded c(c*a), c_{44} und c(c*c*)* in the ferroic monoclinic phase and

* Ultrasonic velocities and their corresponding stiffnesses are denoted by their direction of propagation and polarization in parentheses

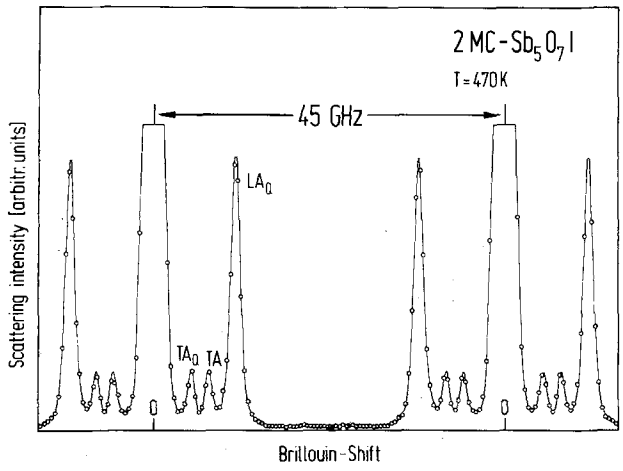

Fig. 5. A typical Brillouin spectrum of Sb_5O_7I which shows two orders of the interference pattern; LA_Q: quasi-longitudinal acoustic phonon; TA, TA_Q: transversal, quasi-transversal acoustic phonon. The strong elastic peak is cut

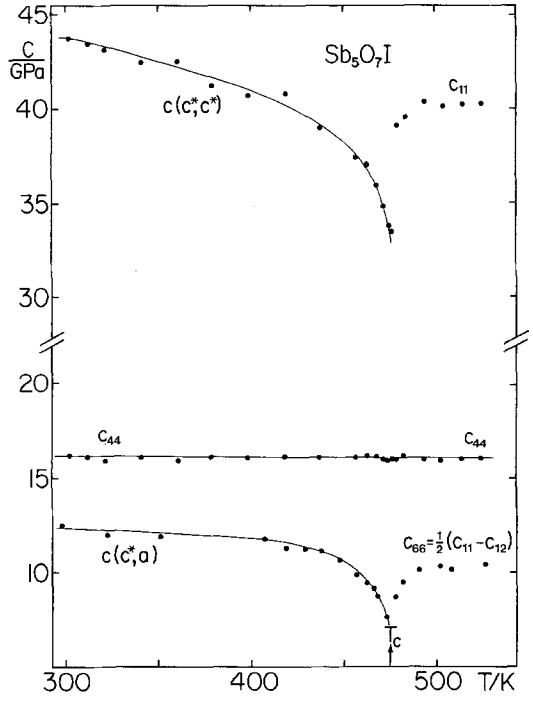

Fig. 6. Temperature dependence of the elastic stiffnesses measured by Brillouin scattering. The full lines represent computer fits similar to Fig. 2. The nomenclature is according to Table 1

$\frac{1}{2}(c_{11}-c_{12})$, c_{44} and c_{11} for the hexagonal high temperature structure. The elastic constants c(c*c*) and c_{11} correspond to quasi-longitudinal and longitudinal elastic waves, respectively. Their magnitudes as function of temperature agree rather well with those determined from the ultrasonic measurements. The quasi-longitudinal (c(c*,c*)) and the transverse waves (c_{44}) showed very significant signals which did not change much at T_c. On the contrary the intensity scattered by the quasi-transverse wave (c(c*,a)) was very weak at room temperature and increased drastically close to T_c. Above T_c the scattering intensity of this shear-wave was again very weak. This is connected with the observation of a rapidly increasing number of domains near T_c, although we started the measurement with a monodomain crystal at room temperature and heated slowly.

In addition we looked for the appearance of a central component around T_c. We found no indication for a reproducible static or dynamic central peak. However, for a thorough investigation of this problem a tandem Fabry-Perot interferometer and selective filtering of the elastic component would be necessary as described by Lyons and Fleury [10].

3. Discussion

Of all the measured elastic functions only c_{44} goes unaffected through the phase transition point T_c. All the others, namely c_{11}, c_{22}, c(c*,c*) and c(c*,a) (in monoclinic notation) experience variations around T_c: c_{22} only a faint dip and a change in slope at T_c, while the rest shows a considerable softening of about 20%.

In the following we are going to discuss the observed effects upon the elastic behaviour by means of a phenomenological expansion of the free-energy density for the coupling between the ordering coordinate Q – below T_c also its expectation value $\eta=\langle Q\rangle$, the order parameter – and the components of the elastic strain e [11]:

$$F_c(e_i,Q_j)=\sum_{\substack{i,j,k,\\ \mathbf{q}}} g_{ijk}e_iQ_j(\mathbf{q})Q_k(-\mathbf{q})$$

$$+\tfrac{1}{2}\sum_{\substack{i,j,k,p,\\ \mathbf{q}}} h_{ijkp}e_ie_jQ_k(\mathbf{q})Q_p(-\mathbf{q})+\ldots \qquad (1)$$

These terms describe cubic and quartic anharmonicity between one or two acoustic phonons in the long-wavelength limit and two components of the ordering coordinate. Starting from the hexagonal phase the ordering coordinate transforms like the irreducible representation M_2 of the factor group of the wavevector $\mathbf{q}_M$ of C_{6h}^2 [4]. The three components of the ordering coordinate Q_j (j=1, 2, 3) belong to the three equivalent wavevectors of the star of $\mathbf{q}_M$. From the symmetric square of the whole star representation $^*M_2$ only the components belonging to A_g and E_{2g} are relevant for the coupling to quasistatic strain. The symmetrized strain components transform like the following irreducible representations of C_{6h}:

$$\underset{A_g}{e_1+e_2} \quad \underset{A_g}{e_3} \quad \underset{E_{1g}}{(e_4,e_5)} \quad \underset{E_{2g}}{(e_6,e_1-e_2)}.$$

So cubic anharmonicity gives a free coupling energy density

$$F_c^{(3)}=[g_1(e_1+e_2)+g_2e_3](Q_1^2+Q_2^2+Q_3^2)$$
$$+g_3[e_6(Q_1^2-Q_2^2)+(e_1-e_2)(2Q_3^2-Q_1^2-Q_2^2)/\sqrt{3}]. \quad (2)$$

Since (e_1+e_2) and e_3 do not break the symmetry of C_{6h}, their corresponding elastic stiffnesses $(c_{11}+c_{12})/2$ and c_{33} should decrease in the hexagonal phase proportional to the specific heat capacity [12]. This is a rather weak effect as demonstrated by the variation of the measured c_{33} above T_c. On the other hand, e_1 and e_2 are symmetry-breaking strains as well as e_6; their stiffnesses c_{11} and $c_{66}=(c_{11}-c_{12})/2$ show a temperature dependence determined by the crossover exponent φ [13]:

$$\Delta c_{ii}\sim(T/T_c-1)^{-(2\varphi+\alpha-2)}. \quad (3)$$

A fit through the few data points of c_{11} originating from longitudinal waves along the monoclinic a- and c*-direction is not very reliable. The values obtained for the exponent $\mu_e=2\varphi+\alpha-2$ are between 0.8 and 1, indicating, however, a marked deviation from the Landau theory [14].

Upon entering the monoclinic phase a formal change of notation has to be made in order to comply with the crystallographic rules. The hexagonal a_3-axis now becomes b; the axis, along which doubling of the unit cell occurs, is called c. As a consequence of the lower symmetry several elastic functions split, namely c_{11} into c_{11} and c_{33}, c_{44} into c_{44} and c_{66}. In addition, several new stiffness components appear, that were zero in the hexagonal phase: c_{15}, c_{25}, c_{35}, and c_{46}. Their appearance indicates that several of the previously pure modes now become quasi-longitudinal or quasi-transverse modes. They are indicated in Table 1 by a subscript "Q".

Both, the splitting and the newly developing components are connected with the ordering and are expected to very like an even power of the order parameter $\eta=\langle Q\rangle$. This effect is similar to the activation of certain Raman lines. The formal description is given by quartic anharmonic interaction and is contained in the second terms of (1). All the 13 stiffness components of the monoclinic system can, in principle, vary in lowest order like:

$$\Delta c_{ij}=h_{ij33}\eta^2$$

within a certain domain, say $\langle Q_3\rangle\neq 0$. In the Landau theory, these quantities have a discontinuity at T_c and a squareroot dependence below T_c:

$$\Delta c_{ij}=\frac{2}{3}h_{ij33}\eta^2(T_c)\left[1+\sqrt{\frac{T_1-T}{T_1-T_0}}\right]. \quad (4)$$

Here T_c is the transition temperature where both phases have equal free energy, and T_1 and T_0 denote the upper and lower stability limit.

In addition there is a contribution to the monoclinic c_{11}, c_{22}, c_{33}, and c_{55} proportional to the specific heat capacity and originating from the cubic anharmonicity described in (2). In the framework of the Landau theory this amounts to:

$$\Delta c_{ij}=-2g_{ij}^2\Big/\left(|a_4|\sqrt{\frac{T_1-T}{T_1-T_0}}\right). \quad (5)$$

The coupling coefficients g_{ij} (in monoclinic notation: $ij=11$, 22, 33, and 55, as well as 12, 23, and 13) are linear combinations of the three coupling parameters g_1, g_2, and g_3, describing cubic anharmonic interactions between strain and order parameter in (2). Their value depends also on the ratio of the various order-parameter components Q_i, which is not known. The fact that both types of spontaneous strain, $\langle e_6\rangle$ and $\langle e_1-e_2\rangle$ (in hexagonal notation) appear [4] indicates that more than one order-parameter component is involved in the ordering. The isotropic fourth-order coefficient in the Landau expansion is denoted by a_4.

We tried to fit a superposition of (4) and (5) to our measured stiffness functions $c(a,a)$, c_{22}, $c(c^*,c^*)$, and $c(c^*,a)$. It turned out that in c_{22} the contribution from (5) is negligibly small (i.e., below the uncertainties calculated from the fit) and that the variation below T_c is dominated by quartic anharmonicity. On the other hand, in $c(a,a)$ and $c(c^*,a)$ the main effect comes from interactions with energy-density fluctuations [(2) and (5)], whereas the contribution from activation is marginal. In $c(c^*,c^*)$ both contributions are detectable. Attempts to fit the experimental curves with a variable exponent always resulted in values close to $\pm 1/2$ within experimental uncertainties. The stability limit of the ordered phase, calculated as the average over the results of 17 different program runs, is $T_1=(482.2\pm 0.5)$ K.

These experimental findings are in good agreement with the predictions made on the basis of possible coupling mechanisms. Both $c(a,a)$ and $c(c^*,c^*)$, containing c_{11} and c_{33} as the main contributions, are affected by a combination of the coupling coefficients g_1 and g_3. On the other hand g_2, belonging to c_{22}, is found to be negligibly small. Quartic anharmonicity acts predominantly on c_{22} and $c(c^*,c^*)$. The experimental observation that $h_{1133}\approx 0$ shows that the splitting of c_{11} and c_{33} in the monoclinic phase is carried by the shift, proportional to the square of the order parameter, in c_{33}. Whether these quartic interactions work directly or via the spontaneous strain cannot be decided at the moment.

For a more quantitative evaluation the single stiffness components have to be calculated from the complicated expressions in Table 1. For this the number of data is insufficient.

4. Summary

The elastic stiffnesses of ferroelastic $2MC-Sb_5O_7I$ have been measured as functions of temperature in both structural phases by combining ultrasonic techniques and Brillouin scattering. The experimental results confirm the view of $2MC-Sb_5O_7I$ being an improper ferroelastic material, where quadratic terms of the zone boundary ordering coordinate couple to elastic deformations and yield the ferroelastic properties of the crystal in the low temperature phase. The observed softening of some elastic functions below T_c could be sufficiently well described by assuming the temperature variation of the order parameter according to the Landau theory of weakly discontinuous phase transitions. This result is in agreement with previous Raman scattering measurements on optical phonons activated by the phase transition [5] and with the temperature dependence of the birefringence in the ferroic phase [6]. Above T_c, however, the temperature variation of the elastic constants, being due to order parameter fluctuations, shows a clear deviation from classical Landau behaviour.

We are indebted to Profs. R. Nitsche and V. Krämer and Dipl. Phys. M. Schuhmacher for providing the samples and many interesting communications on the structural properties of the crystals.

References

1. Krämer, V., Nitsche, R., Schuhmacher, M.: J. Cryst. Growth **24/25**, 179 (1974)
2. Nitsche, R., Krämer, V., Schuhmacher, M., Bussmann, A.: J. Cryst. Growth **42**, 549 (1977)
3. Krämer, V.: Acta cryst. B**31**, 234 (1975)
4. Prettl, W., Rieder, K.H., Nitsche, R.: Z. Phys. B**22**, 48 (1975)
5. Prettl, W., Rieder, K.H.: Phys. Rev. B**14**, 2171 (1976)
6. Jahn, I.R.: private communication
7. "Standards on Piezoelectric Crystals", Proc. IRE **37**, 1378 (1949)
8. Papadakis, E.M.: In: Physical Acoustics, edited by Mason, W.P., Thurston, R.N. (eds.), Vol. **12**, p. 289. New York: Academic Press, 1970
9. Sandercock, J.R.: J. Phys. E: Sci. Instrum. **9**, 566 (1976) We thank Dr. Sandercock for the production of this device
10. Lyons, K.B., Fleury, P.A.: Phys. Rev. B**17**, 2304 (1977)
11. Rehwald, W.: Adv. Phys. **22**, 721 (1973)
12. Rehwald, W., Lang, G.K.: J. Phys. C**8**, 3287 (1975)
13. Bruce, A.D., Aharony, A.: Phys. Rev. B**11**, 478 (1975); and Aharony, A., Bruce, A.D.: Phys. Rev. Lett. **33**, 427 (1974)
14. Henkel, W., Pelzl, J., Höck, K.-H., Thomas, H.: Z. Physik B (to be published)

W. Rehwald
A. Vonlanthen
Laboratories RCA Ltd.
Badenerstr. 569
CH-8048 Zürich
Switzerland

E. Rehaber
W. Prettl
Fakultät für Physik
der Universität Regensburg
Universitätsstraße 31
D-8400 Regensburg
Federal Republic of Germany